

Evidence of Conformational Equilibrium of 1-Ethyl-3-methylimidazolium in Its Ionic Liquid Salts: Raman Spectroscopic Study and Quantum Chemical Calculations

Yasuhiro Umebayashi, Takao Fujimori, Tetsuya Sukizaki, Mitsunori Asada, Kenta Fujii,
Ryo Kanzaki, and Shin-ichi Ishiguro*

Department of Chemistry, Faculty of Science, Kyushu University,
Hakozaki, Higashi-ku, Fukuoka 812-8581, Japan

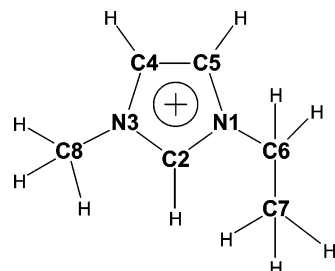
Received: June 27, 2005; In Final Form: August 2, 2005

Raman spectra of liquid 1-ethyl-3-methylimidazolium (EMI^+) salts, $\text{EMI}^+\text{BF}_4^-$, $\text{EMI}^+\text{PF}_6^-$, $\text{EMI}^+\text{CF}_3\text{SO}_3^-$, and $\text{EMI}^+\text{N}(\text{CF}_3\text{SO}_2)_2^-$, were measured over the frequency range 200–1600 cm^{-1} . In the range 200–500 cm^{-1} , we found five bands originating from the EMI^+ ion at 241, 297, 387, 430, and 448 cm^{-1} . However, the 448 cm^{-1} band could hardly be reproduced by theoretical calculations in terms of a given EMI^+ conformer, implying that the band originates from another conformer. This is expected because the EMI^+ involves an ethyl group bound to the N atom of the imidazolium ring, and the ethyl group can rotate along the C–N bond to yield conformers. The torsion energy for the rotation was then theoretically calculated. Two local minima with an energy difference of ca. 2 kJ mol^{-1} were found, suggesting that two conformers are present in equilibrium. Full geometry optimizations followed by normal frequency analyses indicate that the two conformers are those with planar and nonplanar ethyl groups against the imidazolium ring plane, and the nonplanar conformer is favorable. It elucidates that bands at 241, 297, 387, and 430 cm^{-1} mainly originate from the nonplanar conformer, whereas the 448 cm^{-1} band does originate from the planar conformer. Indeed, the enthalpy for conformational change from nonplanar to planar EMI^+ experimentally obtained by analyzing band intensities of the conformers at varying temperatures is practically the same as that evaluated by theoretical calculations. We thus conclude that the EMI^+ ion exists as either a nonplanar or planar conformer in equilibrium in its liquid salts.

Introduction

The 1-alkyl-3-methylimidazolium cation with some simple counteranions forms ionic liquids at room temperature. These room-temperature ionic liquids (RTILs) have attracted attention as noble electrolyte materials and as new media for organic reactions and solvent extraction.^{1,2} A number of studies for the application of RTILs have been carried out, although little is known about their molecular properties as a solvent. Recently, studies revealed that conformers for 1-butyl-3-methylimidazolium (BMI^+) exist in the liquid state, as well as in the crystalline state.^{3,4} For 1-ethyl-3-methylimidazolium (EMI^+),⁵ although crystal structures have been investigated,⁶ no direct information on conformers has been obtained in the liquid state. According to our survey using the Cambridge Structural Database (CDS),⁷ there are 35 crystal structure data for the EMI^+ salts.⁶ By looking at the ethyl group of EMI^+ (Chart 1), the C2–N1–C6–C7 dihedral angle θ changes depending on the temperature, the kind of counteranions, and the molecular arrangement in crystals, and it revealed that the value, the number of molecules with the dihedral angle θ , distributes at around $\theta = 15^\circ$ and 105° , as seen in Figure 1. This implies that two conformers are favorable in the crystalline state. However, according to quantum chemical calculations for the single EMI^+ molecule,^{8,9} it is still not clear whether both conformers are really favorable, as the energy potential surface for rotation of the ethyl group strongly depends on the level of molecular orbital (MO) theory and the basis set employed. Molecular dynamics simulations for a EMI^+

CHART 1: Numbering of the Skeleton Atoms for the 1-Ethyl-3-methylimidazolium Cation



salt in the liquid state have also been reported,^{10–12} but no considerations have been made on the conformers.

So far, we have investigated conformational change of molecular solvents upon their coordination to the metal ion in solution by Raman spectroscopy, quantum mechanical calculations, etc.¹³ Our techniques must also be useful for elucidating conformational equilibria of RTILs in the liquid state. Although the presence of conformers has been established for EMI^+ in the crystalline state as mentioned above, no direct experimental evidence has been obtained in the liquid state. Here, we show spectroscopic evidence for the presence of two conformers of 1-ethyl-3-methylimidazolium in the liquid state by Raman spectroscopy and quantum chemical calculations.

Experimental Section

Materials. 1-Ethyl-3-methylimidazolium tetrafluoroborate (BF_4^-), hexafluorophosphate (PF_6^-), and bis[(trifluoromethyl)-

* Corresponding author. E-mail: analssc@mbox.nc.kyushu-u.ac.jp.

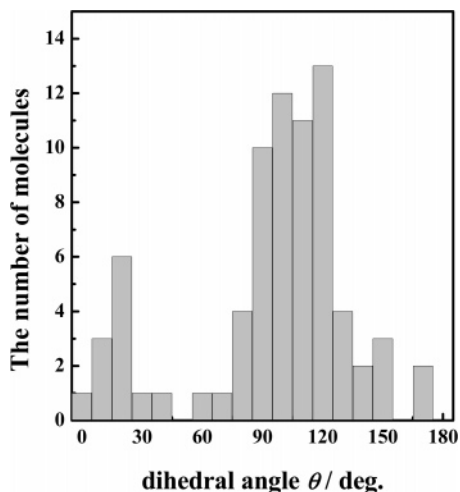


Figure 1. Distribution of the C2–N1–C6–C7 dihedral angle in 1-ethyl-3-methylimidazolium salt crystals. Data were taken from the CSD database. See ref 6.

sulfonyl]imide ($\text{N}(\text{CF}_3\text{SO}_2)_2^-$, TFSI $^-$) of spectroscopic grade (Nippon Synthetic Chemical Industry) and 1-ethyl-3-methylimidazolium trifluoromethanesulfonate (CF_3SO_3^- , TF $^-$) (Tokyo Kasei Kogyo) were used without further purification. Water content checked by a Karl Fischer test was less than 100 ppm for all salts examined here. All materials were treated in a high-performance glovebox (Miwa), in which water and oxygen contents were kept at less than 1 ppm.

Raman Spectroscopy. Raman spectra were obtained using a Fourier transform (FT) Raman spectrometer (Perkin-Elmer GX-R) equipped with a Nd/YAG laser operating at 1064 nm. The laser power was at 800–1000 mW and was kept constant throughout the measurements. The optical resolution was 4 cm^{-1} , and spectral data were accumulated 512–1024 times to obtain a sufficient signal-to-noise ratio. The sample liquid in a quartz cell was stirred and thermostated at a given temperature within ± 0.3 K. The sample room was filled with dry N_2 gas to avoid condensation of moisture on the surface of the cell. No appreciable damage was detected for the sample materials after the measurement.

Raman spectra obtained over a given frequency range were deconvoluted to extract single Raman bands. A single Raman band is assumed to be represented as a pseudo-Voigt function, $f_V(v) = \gamma f_L(v) + (1 - \gamma) f_G(v)$, where $f_L(v)$ and $f_G(v)$ stand for Lorentzian and Gaussian components, respectively, and the parameter γ ($0 < \gamma < 1$) is the fraction of the Lorentzian component. To avoid uncertainty in obtaining the γ value of the peaks, the values were fixed to those obtained at the lowest temperature. The intensity I of a single Raman band is evaluated according to $I = \gamma I_L + (1 - \gamma) I_G$, where I_L and I_G denote integrated intensities of the Lorentzian and Gaussian components, respectively. A nonlinear least-squares curve-fitting program, RAMCAL, based on the Marquardt–Levenberg algorithm,^{14,15} was developed in our laboratory and used throughout the analyses.

DFT and ab Initio Calculations. DFT and ab initio calculations were carried out using the Gaussian 03 program package.¹⁶ The potential energy profile for conformational change of the EMI^+ ion was obtained for the first time by Hartree–Fock level ab initio calculations using 6-311+G(d,p) and aug-cc-pvDZ¹⁷ basis sets and was then corrected for the electron correlation effect by means of ab initio Møller–Plesset second-order perturbation theory¹⁸ (MP2) and density functional theory according to Becke's three-parameter hybrid method¹⁹

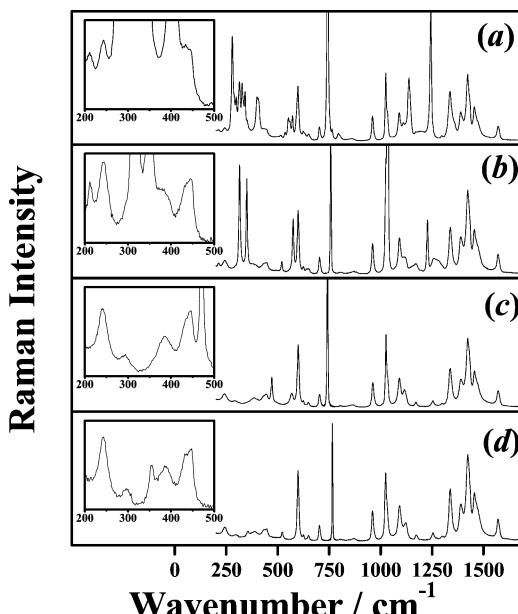


Figure 2. Raman spectra of liquid 1-ethyl-3-methylimidazolium salts, CTFSI $^-$ (a), EMI^+TF^- (b), $\text{EMI}^+\text{PF}_6^-$ (c), and $\text{EMI}^+\text{BF}_4^-$ (d), measured at 298 K (TFSI $^-$, TF $^-$, and BF $^-$ salts) and at 333 K (PF $_6^-$).

with LYP correlation²⁰ (B3LYP). The energy profile showed two local minima, and to confirm that the local minima were not saddle points, full geometry optimizations and normal frequency analyses were carried out at each optimized geometry.

Results and Discussion

Raman Spectra. Raman and IR spectra of liquid $\text{EMI}^+\text{PF}_6^-$ have been reported over the range 500–3500 cm^{-1} by Talaly et al.⁹ Theoretical calculations indicate that the nonplanar EMI^+ gives the lowest energy.^{8–11} On the basis of theoretical calculations, Talaly et al. assigned observed bands at 598, 741, 1340, 1421, 1452, 1572, 2878, 2917, 2942, 2970, 3180, and 3115 cm^{-1} to intramolecular vibrations of the nonplanar EMI^+ . Although they did not give spectra in the range $< 500 \text{ cm}^{-1}$, they predicted that the EMI^+ shows the $\text{CH}_2(\text{N})$ bend vibration at 245 cm^{-1} and shows three CCH bend + $\text{CH}_3(\text{N})$ bend vibrations at 301, 395, and 427 cm^{-1} . We measured Raman spectra of liquid $\text{EMI}^+\text{TFSI}^-$, EMI^+TF^- , $\text{EMI}^+\text{PF}_6^-$, and $\text{EMI}^+\text{BF}_4^-$ over the range 200–1600 cm^{-1} , as shown in Figure 2. The obtained spectrum of $\text{EMI}^+\text{PF}_6^-$ in the range $> 500 \text{ cm}^{-1}$ is in good agreement with that previously reported by Talaly et al.⁹ With regard to the range 200–500 cm^{-1} , we found five Raman bands originating from the EMI^+ at 241, 297, 387, 430 (shoulder of the 448 cm^{-1} band), and 448 cm^{-1} , although some of them overlapped with those of counteranions. The first four Raman bands are assigned to those predicted by Talaly et al., whereas the 448 cm^{-1} band is not reproduced by the theoretical calculation.

According to Turner et al.,⁸ who carried out ab initio calculations for the 1-alkyl (methyl, ethyl, propyl, and butyl)-3-methylimidazolium ion on the basis of HF and MP2 theories with STO-3G, 3-21G, 6-31G*, and 6-31+G* basis sets, the EMI^+ conformers with nonplanar C_1 and planar C_s geometries are present in equilibrium. The planar conformer has a slightly higher energy (2–4 kJ mol $^{-1}$). This implies that the 448 cm^{-1} band originates from the planar EMI^+ conformer. However, note that, with the planar EMI^+ , one imaginary frequency mode appears according to the MP2 level calculation. This indicates that the potential energy surface (PES) is so flat that no definite

TABLE 1: Selected Structural Parameters, Molecular Properties, and Relative Energies for Nonplanar (np) and Planar (p) Conformers of the 1-Ethyl-3-methylimidazolium Cation^a and Enthalpies of Conformational Change from Nonplanar to Planar^b

		6-311+G(d,p)						aug-cc-PVDZ					
		HF		MP2		B3LYP		HF		MP2		B3LYP	
		p	np	p	np	p	np	p	np	p	np	p	np
bond lengths (Å)	C2–H9	1.068	1.070	1.078	1.080	1.076	1.078	1.073	1.074	1.085	1.087	1.081	1.083
	C4(5)–H	1.068	1.068	1.080	1.080	1.077	1.077	1.073	1.073	1.087	1.087	1.083	1.083
	C8–H	1.080	1.080	1.090	1.090	1.089	1.090	1.085	1.085	1.097	1.097	1.095	1.095
	C6–H	1.082	1.082	1.092	1.092	1.092	1.091	1.086	1.086	1.100	1.099	1.097	1.096
	C7–H	1.085	1.084	1.093	1.092	1.092	1.092	1.089	1.089	1.100	1.100	1.098	1.097
	C2–N1	1.314	1.313	1.344	1.344	1.337	1.336	1.317	1.316	1.351	1.350	1.339	1.339
	C2–N3	1.315	1.314	1.344	1.344	1.338	1.337	1.318	1.317	1.351	1.351	1.340	1.340
	C4–N3	1.378	1.378	1.375	1.375	1.381	1.382	1.378	1.379	1.379	1.379	1.382	1.382
	C5–N1	1.379	1.378	1.376	1.375	1.383	1.382	1.379	1.378	1.380	1.379	1.383	1.382
	C4–C5	1.340	1.341	1.375	1.376	1.361	1.345	1.346	1.346	1.385	1.386	1.366	1.367
	N3–C8	1.466	1.466	1.470	1.471	1.470	1.471	1.466	1.466	1.474	1.474	1.469	1.470
	N1–C6	1.482	1.478	1.484	1.479	1.488	1.484	1.481	1.477	1.487	1.482	1.487	1.482
	C6–C7	1.518	1.522	1.519	1.522	1.520	1.519	1.522	1.523	1.527	1.521	1.526	1.526
angles (deg)	C4–N3–C2	108.1	108.0	108.9	108.8	108.5	108.4	108.1	108.0	109.1	109.0	108.5	108.4
	C5–N1–C2	107.9	107.9	108.7	108.8	108.3	108.3	107.9	108.0	108.8	108.9	108.3	108.4
	C4–C5–N1	106.9	107.2	107.2	107.0	107.3	107.2	107.3	107.1	107.1	107.0	107.3	107.2
	C5–C4–N3	106.9	107.0	106.9	107.0	107.0	107.1	106.9	107.0	106.8	106.9	107.0	107.0
	C8–N3–C2	126.2	126.3	125.4	125.5	125.8	125.9	126.1	126.2	125.3	125.4	125.8	125.9
	C8–N3–C4	125.7	125.7	125.7	125.7	125.7	125.7	125.7	125.7	125.6	125.6	125.7	125.7
	C6–N1–C2	128.0	126.1	126.8	125.4	127.2	125.8	127.9	126.0	126.6	125.3	127.2	125.7
	C6–N1–C5	124.1	126.0	124.5	125.8	124.5	125.9	124.2	126.0	124.6	125.6	124.5	125.8
	N1–C6–C7	113.4	112.3	112.6	111.0	113.6	112.4	113.5	112.3	112.4	111.0	113.5	112.3
dihedral angle (deg)	C2–N1–C6–C7	0.0	107.1	0.0	110.4	0.0	104.6	0.0	105.7	0.0	101.5	0.0	103.1
dipole moment ((10 ⁻³⁰) cm)	N1–C5–C4–N3	0.0	0.0	0.2	0.0	0.1	0.0	0.1	0.0	0.3	0.0	0.2	
	N1–C2–N3–C8	180.0	180.0	180.0	178.6	180.0	179.6	180.0	179.6	180.0	178.8	180.0	179.6
		3.85	6.10	3.94	5.58	3.78	5.46	3.78	5.95	3.85	5.30	3.71	5.34
dipole moment (D)		1.16	1.83	1.18	1.67	1.13	1.64	1.13	1.78	1.15	1.59	1.11	1.60
$E((10^3) \text{ kJ mol}^{-1})$		-898.96	-898.96	-902.13	-902.13	-904.84	-904.84	-898.84	-898.84	-901.96	-901.96	-904.70	-904.70
EZPC ((10 ³) kJ mol ⁻¹)		-899.43	-899.43	-902.58	-902.58	-905.29	-905.29	-899.31	-899.31	-902.40	-902.40	-905.14	-905.14
$\Delta E(\text{kJ mol}^{-1})$		3.2	3.6	2.4	2.8	2.2	2.2						
$\Delta H(\text{kJ mol}^{-1})$		3.6	2.6	3.2	2.6								
$\Delta S(\text{J K}^{-1}\text{mol}^{-1})$		2.0	6.1	-0.8	1.1								
$\Delta G(\text{kJ mol}^{-1})$		3.0	0.8	3.4	2.3								
$\Delta_{\text{iso}}H^\circ(\text{kJ mol}^{-1})$	I_{448}/I_{387}		2.1(2) (EMI ⁺ TF ⁻)					2(2) (EMI ⁺ BF ₄ ⁻)					
	I_{448}/I_{430}		2.0(1) (EMI ⁺ TF ⁻)					4(2) (EMI ⁺ BF ₄ ⁻)					

^aStructural parameters, molecular properties, and relative energies were obtained by quantum chemical calculations. ^b Enthalpies of conformational change were experimentally obtained.

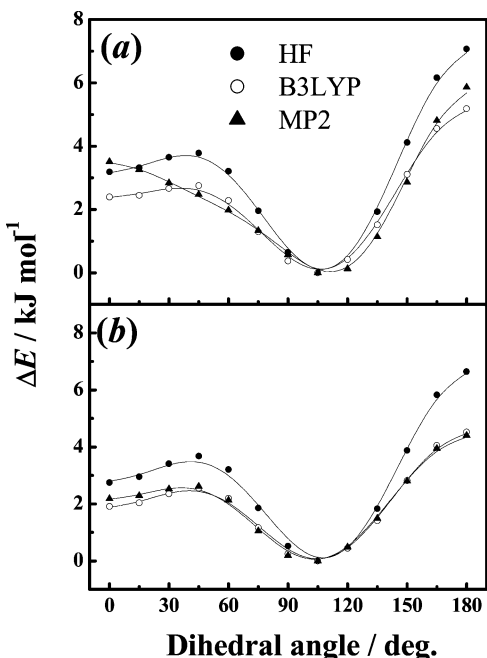
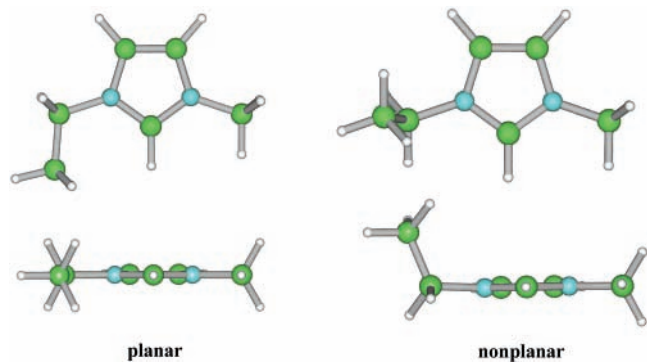


Figure 3. Potential energy surfaces for torsion of the C2–N–C6–C7 dihedral angle of the EMI⁺ ion calculated using the 6-311+G(d,p) (a) and aug-cc-pvdZ (b) basis sets.

conclusion is drawn for the presence of the planar EMI⁺ conformer. To clarify this, we also carried out theoretical calculations as shown in the following section.

CHART 2: Optimized Geometries for Nonplanar and Planar Conformers of the EMI⁺ Cation



Torsion Energy Potential Surface of the EMI⁺. The torsion energy potential surface has been calculated for the C5–N1–C6–C7 dihedral angle of the EMI⁺ (see Chart 1). According to Lopes et al.,¹⁰ MP2/cc-pvTZ(-f)//HF/6-31G(d) calculations gave two local minima at angles corresponding to the nonplanar and planar conformers. On the other hand, according to Liu et al.,¹¹ MP2/6-31+G(d)//HF/6-31+G(d) calculations gave only a single local minimum. The conclusion thus depends on the employed basis sets, particularly whether the basis set involves a diffuse function or not. Also, the HF level calculation gave two local minima using the 6-31G(d) basis set and a single minimum using the 6-31+G(d) basis set. This implies that not only the level of theory but also the basis set influences the PES estimate.

To estimate a more reliable PES, the larger basis set must be needed. Thus, we calculated the PES on the basis of the HF theory using the 6-311+G(d,p) and aug-cc-pvdZ basis sets. Using the same basis sets, we also examined B3LYP and MP2 calculations, in which the electron correlation effect is taken into account. The PESs thus calculated are shown in Figure 3. All except for the MP2/6-311+G(d,p) calculation gave two local minima at angles 0° and 110°. We thus propose that two EMI⁺ conformers exist with respect to the C5—N1—C6—C7 dihedral angle and the planar and nonplanar conformers, and the nonplanar conformer is preferred to the planar one.

Optimized Geometries and Calculated Raman Spectra. Full geometry optimizations followed by normal frequency analyses were then performed for the planar and nonplanar EMI⁺ conformers. For both conformers, optimized geometries with no imaginary frequency were obtained using the aug-cc-pvdZ basis set. Optimized geometries are depicted in Chart 2. Selected structural parameters (bond lengths and angles) and molecular parameters (dipole moments and relative energies) are listed in Table 1. The partial atomic charges evaluated by means of Mulliken,²¹ atomic polar tensor,²² and ChelpG²³

methods are given as Supporting Information. No significant difference was found in any structural parameter within all levels of calculation employed here. All levels of theory gave a larger dipole moment for the nonplanar conformer than for that of the planar conformer, implying that the nonplanar conformer is even more preferred to the planar one in dielectric solvents and ionic liquids.

Predicted Raman bands are listed in Table 2, together with observed ones. Calculated band frequencies are plotted against observed ones over the range 200–1600 cm⁻¹ (given as Supporting Information) to give a scaling factor. Scaling factors are also listed in Table 2. The HF, MP2, and B3LYP levels of theory using the 6-311+G(d,p) basis set gave scaling factors of 0.914, 0.985, and 0.989, respectively. On the other hand, the HF, MP2, and B3LYP levels of theory using the aug-cc-pvdZ basis set gave the values of 0.914, 0.995, and 0.992, respectively. As the MP2/aug-cc-pvdZ calculation gives the best prediction of band frequencies, we will discuss the results obtained by this calculation in the following section.

The nonplanar EMI⁺ gives five Raman active vibrations at 209.4 ($I_{\text{Raman}} = 0.16$), 230.1 (0.76), 291.6 (0.39), 379.9 (1.55),

TABLE 2: Observed Raman Bands and Predicted Frequencies of the 1-Ethyl-3-methylimidazolium Cation

ν_{obs}	HF						6-311+G(d,p) MP2						B3LYP					
	planar			nonplanar			planar			nonplanar			planar			nonplanar		
	ν_{calcd}	I_{ir}	I_{Raman}															
241(m)	34.1	0.66	0.67	50.7	0.36	0.76	-57.0	0.36	0.91	28.3	0.11	0.24	21.2	0.39	0.84	46.4	0.26	1.06
297(w)	93.7	0.28	0.09	92.5	0.22	0.12	-39.6	0.13	0.15	40.4	0.27	0.90	66.7	0.24	0.19	71.7	0.15	0.25
387(m)	179.6	3.44	0.71	145.3	1.08	1.32	157.1	4.40	0.85	128.7	1.61	1.54	168.2	3.70	0.81	135.4	1.30	1.66
430(sh)	199.5	0.55	0.30	222.2	0.18	0.03	189.4	0.59	0.33	208.8	1.86	0.57	187.0	0.56	0.40	208.7	0.23	0.07
448(m)	263.0	0.55	1.15	245.6	1.90	1.13	222.8	0.72	1.03	214.2	0.64	0.44	247.7	0.70	0.87	232.8	1.95	1.00
600(vs)	325.6	0.22	0.10	309.6	0.11	0.21	307.7	0.32	0.05	292.5	0.24	0.30	299.5	0.17	0.14	292.1	0.20	0.32
626(w)	376.0	0.34	0.33	399.1	0.35	1.52	353.3	0.47	0.35	369.2	0.59	1.29	355.3	0.55	0.42	377.9	0.38	1.74
650(w)	471.7	1.08	3.07	453.0	0.30	1.05	446.2	0.94	3.61	424.5	0.33	1.41	447.0	0.94	3.98	425.5	0.40	1.19
704(m)	626.6	2.36	7.96	628.2	3.72	7.95	573.9	0.13	0.05	584.1	0.88	2.43	590.8	1.34	6.25	591.7	2.34	6.30
805(vw)	677.6	31.93	0.04	679.4	21.14	0.25	594.7	11.72	0.00	596.5	5.94	4.40	631.5	2.47	0.17	632.6	10.96	0.17
872(vw)	682.6	3.28	0.34	707.9	18.35	0.50	595.5	1.06	7.45	635.4	11.50	0.84	634.9	20.65	0.02	660.2	15.58	0.22
960(s)	748.3	16.03	2.94	738.8	18.26	2.61	707.9	4.70	0.33	705.2	8.95	2.54	705.9	7.07	2.54	698.2	9.63	2.51
1025(vs)	852.9	45.23	0.10	852.4	36.74	0.05	710.9	7.03	2.63	709.9	6.62	0.45	755.0	29.93	0.16	753.1	27.78	0.18
1033(sh)	869.5	5.01	0.13	857.0	11.34	0.12	768.9	71.77	0.04	773.9	72.56	0.12	807.3	1.28	0.19	802.6	1.40	0.06
1095(s)	1001.8	0.01	1.72	1001.1	0.12	2.04	806.5	0.22	0.10	806.8	0.68	0.06	840.7	37.03	0.24	834.2	36.85	0.27
1122(m)	1014.5	15.23	0.25	1011.6	15.12	0.27	818.3	5.73	0.20	809.6	0.48	0.13	882.4	0.05	0.49	881.1	0.05	0.69
1173(w)	1037.7	0.70	4.56	1025.4	1.52	7.93	984.3	0.92	3.29	979.1	1.76	5.71	974.0	2.15	3.02	962.2	3.55	5.89
1254(w)	1104.9	0.24	6.98	1099.5	0.08	7.66	1042.1	0.37	6.87	1042.5	0.10	6.16	1036.6	1.25	5.82	1036.1	0.54	7.68
1298(w)	1116.8	1.88	4.03	1118.7	1.64	3.57	1060.7	0.47	8.42	1054.1	1.72	8.00	1047.7	0.54	4.96	1042.7	1.13	3.56
1336(vs)	1188.6	2.77	5.18	1184.7	2.24	5.47	1110.9	3.36	5.79	1113.0	1.50	1.71	1099.0	3.67	5.87	1099.1	3.47	4.38
1388(s)	1190.1	2.01	6.78	1191.9	2.07	1.75	1126.2	5.29	6.83	1121.7	8.81	4.41	1105.6	0.48	3.50	1102.3	2.47	2.95
1411(sh)	1211.9	8.52	2.43	1210.0	7.92	2.79	1131.0	7.60	1.44	1131.1	6.89	6.29	1126.6	12.12	2.69	1124.7	8.50	1.88
1425(vs)	1251.0	0.15	0.97	1232.9	2.77	2.46	1160.1	0.03	0.68	1151.9	1.30	1.77	1148.8	0.13	0.57	1135.9	3.31	2.50
1455(s)	1266.6	2.29	0.08	1251.8	0.62	0.79	1179.2	2.19	0.11	1162.7	0.75	0.75	1163.0	1.70	0.05	1149.9	0.01	0.46
1471(sh)	1269.0	159.80	3.89	1274.6	174.05	2.81	1193.9	91.85	1.81	1198.4	91.32	1.59	1169.5	104.66	2.48	1175.5	109.57	1.62
1571(m)	1393.6	30.60	2.17	1375.8	1.05	3.19	1285.8	3.45	0.80	1278.9	0.46	2.87	1283.7	7.76	0.74	1270.3	0.03	2.69
1427.8	2.92	5.76	1423.1	0.41	1.48	1329.6	2.33	5.32	1318.5	0.97	1.64	1322.5	1.99	5.41	1311.4	0.58	1.08	
1429.7	11.61	6.65	1452.0	13.70	11.47	1355.6	15.73	3.77	1372.8	14.50	23.63	1326.9	9.84	11.63	1342.6	9.50	28.26	
1470.6	31.21	7.30	1501.6	18.36	0.99	1379.0	23.57	22.73	1396.9	14.03	4.12	1358.8	26.75	18.13	1384.9	11.87	0.30	
1524.3	3.66	4.08	1522.5	13.53	6.17	1422.8	9.06	12.41	1421.6	1.61	19.05	1409.0	1.98	11.65	1411.0	5.05	18.39	
1549.6	8.86	16.34	1553.7	12.46	1.16	1439.0	5.02	6.06	1439.2	8.91	0.85	1421.5	10.53	8.35	1428.2	6.82	2.09	
1576.3	26.55	14.26	1571.9	0.35	46.61	1459.6	12.99	1.53	1466.5	1.58	2.37	1440.8	11.98	16.05	1437.2	2.14	22.03	
1587.6	2.00	16.50	1583.0	22.51	7.56	1479.6	2.80	4.46	1479.4	6.34	5.10	1464.1	2.75	5.47	1461.1	8.33	6.87	
1601.1	15.21	7.95	1601.2	14.60	8.15	1497.5	15.47	7.71	1499.7	14.82	8.11	1484.6	16.92	8.01	1484.1	16.27	8.22	
1613.8	12.72	9.47	1607.1	8.22	9.35	1513.4	13.90	8.98	1507.4	6.07	12.50	1498.3	14.08	9.08	1491.1	7.47	14.11	
1621.5	2.25	9.36	1609.2	8.95	12.49	1520.3	6.20	13.67	1513.9	18.24	9.47	1501.7	5.54	13.35	1494.4	16.77	9.02	
1631.8	9.24	13.66	1628.4	16.08	2.01	1529.0	0.70	2.15	1523.0	11.16	0.75	1508.5	0.88	3.46	1509.0	15.65	0.90	
1634.9	8.02	9.26	1631.4	12.72	14.80	1535.1	9.37	11.70	1534.6	9.43	10.90	1510.9	11.50	13.78	1510.4	10.10	13.59	
1753.1	105.14	4.91	1748.8	96.88	4.08	1594.2	10.84	3.63	1587.9	8.75	4.53	1600.0	62.74	1.58	1594.6	57.79	2.29	
1758.3	45.67	7.28	1755.5	71.03	6.24	1622.6	65.24	0.25	1619.7	76.44	0.32	1607.2	14.37	5.22	1603.7	26.57	4.11	
3178.8	7.69	125.57	3182.2	6.91	133.37	3089.3	3.04	149.42	3089.7	2.04	150.80	3042.2	4.01	160.51	3046.3	3.00	159.60	
3215.9	10.76	144.19	3216.5	10.64	144.51	3111.6	3.08	154.67	3111.9	3.10	153.92	3068.6	1.22	219.60	3069.3	3.50	174.86	
3228.2	8.35	97.48	3233.0	7.50	88.10	3120.2	3.42	92.95	3123.0	4.59	84.59	3068.9	7.11	51.53	3078.9	5.52	86.25	
3243.5	10.57	63.56	3249.6	9.32	65.02	3173.7	1.10	77.45	3176.5	0.99	72.67	3100.6	1.71	86.21	3110.0	2.41	77.63	
3265.7	10.25	100.23	3261.9	17.06	90.75	3188.6	1.87	79.84	3188.8	3.31	78.07	3122.5	8.70	10.81	3122.1	6.15	95.33	
3281.7	11.77	30.25	3287.9	13.11	22.48	3193.3	4.82	6.71	3196.8	5.66	4.68	3123.3	3.05	101.43	3133.9	8.23	9.37	
3304.6	2.60	58.12	3305.5	2.44	57.73	3218.1	0.00	54.50	3218.5	0.01	54.32	3148.6	0.29	63.54	3149.8	0.23	62.95	
3312.9	3.15	43.69	3313.6	3.01	44.46	3226.0	0.10	40.25	3226.7	0.06	40.82	3164.4	0.46	43.76	3164.8	0.40	44.89	
3426.1	16.17	35.82	3426.5	20.39	26.83	3299.4	16.46	41.04	3300.8	16.15	38.44	3273.4	16.2					

TABLE 2: Continued

ν_{obs}	HF						aug-cc-pvDZ MP2						B3LYP					
	planar			nonplanar			planar			nonplanar			planar			nonplanar		
	ν_{calcd}	I_{ir}	I_{Raman}															
241(m)	42.1	0.58	0.52	47.3	0.36	0.89	27.7	0.23	0.67	39.9	0.26	1.28	34.0	0.33	0.69	45.5	0.26	1.25
297(w)	93.6	0.26	0.05	89.3	0.19	0.06	53.4	0.22	0.18	54.0	0.12	0.11	70.2	0.22	0.15	74.1	0.13	0.16
387(m)	178.7	3.15	0.63	143.2	0.95	1.37	170.8	3.97	0.74	130.7	1.27	1.68	171.5	3.39	0.71	134.6	1.14	1.70
430(sh)	199.6	0.55	0.47	221.6	0.14	0.08	190.6	0.62	0.55	209.4	0.18	0.16	188.8	0.58	0.60	206.8	0.15	0.13
448(m)	258.6	0.51	0.82	241.8	1.76	0.84	247.8	0.59	0.67	230.1	2.19	0.76	249.6	0.63	0.62	233.5	1.84	0.78
600(vs)	330.0	0.21	0.08	309.9	0.13	0.27	317.3	0.27	0.08	291.6	0.29	0.39	302.5	0.17	0.13	291.0	0.24	0.42
626(w)	375.5	0.33	0.35	399.6	0.30	1.62	352.0	0.49	0.47	379.9	0.44	1.55	355.9	0.51	0.52	380.2	0.31	1.83
650(w)	471.3	0.92	3.20	452.1	0.31	1.06	443.6	0.79	3.81	418.7	0.28	1.21	447.3	0.78	4.09	425.2	0.36	1.19
704(m)	626.9	2.26	8.49	628.3	3.35	8.42	591.1	1.04	8.34	593.6	1.48	8.22	592.0	1.24	6.89	593.7	2.05	6.93
805(vw)	676.1	5.69	0.29	677.3	15.55	0.23	617.6	0.00	0.05	625.1	3.87	0.06	632.4	0.22	0.20	634.8	8.90	0.15
872(vw)	679.2	24.76	0.10	705.1	18.65	0.48	635.5	14.73	0.00	656.8	14.78	0.17	639.0	20.84	0.01	662.5	15.45	0.25
960(s)	748.3	15.50	2.38	739.3	17.93	2.20	705.5	6.84	2.13	701.0	8.90	2.22	707.7	6.64	2.11	701.3	8.95	2.08
1025(vs)	852.3	38.83	0.13	848.1	9.45	0.15	729.8	4.72	0.44	726.3	4.54	0.47	762.0	27.89	0.13	759.0	25.54	0.18
1033(sh)	862.7	10.04	0.22	853.4	37.78	0.15	786.5	44.43	0.13	790.6	66.63	0.10	799.8	0.27	0.35	794.7	1.50	0.13
1095(s)	984.4	0.01	2.13	985.3	0.04	2.31	808.0	24.70	0.26	794.4	1.73	0.08	846.2	37.98	0.17	838.8	37.43	0.27
1122(m)	1010.6	16.67	0.33	1005.7	16.77	0.36	825.2	0.15	0.15	828.7	0.06	0.27	874.0	0.06	0.67	873.2	0.04	0.83
1173(w)	1038.6	0.60	4.44	1027.8	1.72	7.17	974.7	0.84	2.97	969.5	2.29	4.79	972.6	1.70	2.82	962.9	3.51	5.18
1254(w)	1104.9	0.33	7.82	1100.7	0.10	8.72	1034.7	0.33	6.65	1034.2	0.05	4.45	1036.0	1.08	6.34	1036.9	0.38	7.04
1298(w)	1117.9	2.01	3.80	1117.4	1.43	2.98	1055.4	0.42	10.57	1049.2	1.70	11.05	1050.5	0.62	5.73	1043.7	1.21	4.86
1336(vs)	1183.3	4.47	7.54	1180.3	3.92	6.55	1097.7	4.81	5.54	1098.8	2.24	1.54	1094.7	4.87	5.94	1095.3	4.71	3.96
1388(s)	1186.2	1.07	4.39	1186.4	1.65	1.52	1114.6	1.98	5.84	1109.9	8.18	7.02	1102.7	0.42	2.79	1097.6	2.88	5.21
1411(sh)	1207.2	7.17	2.83	1204.6	6.73	3.40	1122.0	10.17	2.32	1122.1	8.28	6.47	1123.4	10.93	3.34	1121.1	5.88	1.88
1425(vs)	1242.3	0.04	0.30	1225.6	1.99	2.55	1147.2	0.03	0.16	1131.0	0.60	1.97	1142.1	0.16	0.14	1129.4	3.95	3.21
1455(s)	1258.6	1.72	0.04	1242.8	0.33	0.27	1160.2	1.46	0.03	1148.2	0.17	0.18	1155.8	1.20	0.03	1142.9	0.00	0.14
1471(sh)	1267.5	149.90	3.81	1272.2	163.00	2.86	1182.5	85.73	2.11	1185.7	83.45	1.63	1171.6	96.75	2.62	1176.6	99.45	1.69
1571(m)	1387.6	28.09	2.00	1366.5	0.84	2.29	1269.1	3.18	1.10	1258.7	0.58	2.18	1277.8	7.78	0.96	1260.9	0.04	2.06
1416.3	2.05	3.18	1416.8	0.26	1.06	1312.2	1.65	2.85	1300.2	0.95	0.80	1308.7	1.53	3.21	1305.7	0.76	0.59	
1427.3	13.60	6.00	1450.6	13.33	10.03	1343.5	22.06	1.73	1360.6	17.58	20.19	1329.8	13.72	8.37	1346.7	10.77	27.82	
1467.4	29.68	6.23	1489.2	22.09	0.58	1364.5	18.77	25.24	1372.7	10.55	8.81	1355.3	22.07	19.50	1372.5	10.78	0.76	
1514.7	1.99	1.42	1518.3	5.38	5.21	1400.6	8.51	4.72	1406.2	7.02	0.47	1401.3	5.36	0.56	1403.4	4.89	2.43	
1539.4	11.34	13.42	1537.6	14.24	0.98	1421.0	4.54	14.04	1415.8	1.39	17.53	1411.9	8.19	14.79	1414.8	5.72	15.79	
1564.2	24.58	6.34	1564.9	8.77	12.04	1440.1	11.73	0.82	1444.1	6.81	1.92	1434.1	9.86	18.25	1437.7	0.58	15.84	
1579.1	0.08	25.74	1572.6	12.38	37.58	1457.3	0.82	2.90	1462.6	1.73	5.85	1449.7	0.93	7.48	1447.2	7.51	13.13	
1581.1	13.43	5.10	1580.8	13.17	5.34	1476.8	13.37	5.21	1476.8	12.91	5.63	1461.8	14.40	5.64	1461.3	14.12	5.91	
1596.1	10.43	5.77	1586.2	9.75	4.71	1491.5	11.06	5.69	1481.0	9.27	9.57	1475.2	11.12	6.06	1466.1	4.35	10.45	
1601.6	1.17	5.43	1588.2	3.01	11.03	1492.9	4.72	9.76	1482.1	7.90	5.07	1479.5	2.72	7.23	1467.0	12.29	5.25	
1613.9	6.09	10.79	1611.2	14.70	2.16	1500.7	0.23	1.53	1497.9	11.18	1.31	1489.8	1.27	4.30	1489.6	15.31	3.67	
1619.6	9.71	11.63	1614.1	11.09	15.22	1509.7	9.06	8.83	1509.6	7.90	7.66	1492.0	10.26	12.93	1491.4	7.97	9.90	
1751.4	105.61	4.19	1746.9	95.49	4.48	1585.6	8.05	6.05	1580.6	7.36	5.86	1603.1	57.60	1.53	1596.9	48.37	3.05	
1756.4	31.62	10.81	1753.7	58.62	7.75	1609.8	57.17	0.21	1608.4	66.37	0.38	1607.3	12.95	7.05	1605.1	30.15	4.44	
3182.4	7.66	139.43	3186.0	6.19	146.62	3076.8	3.39	168.86	3077.5	1.88	168.24	3047.6	4.22	171.86	3051.3	2.64	171.70	
3218.5	10.29	162.05	3219.2	10.07	162.77	3101.8	2.85	180.34	3102.1	2.84	177.81	3072.5	3.31	196.90	3072.9	3.19	193.98	
3232.8	8.89	106.98	3238.8	7.59	93.98	3108.7	3.58	103.71	3114.2	4.36	92.16	3077.6	4.64	108.35	3088.2	5.23	93.93	
3252.7	10.25	57.13	3259.0	9.67	57.30	3164.4	1.31	71.88	3168.9	1.62	65.45	3114.0	2.20	77.98	3122.9	3.02	68.26	
3278.8	10.20	96.41	3273.4	16.36	38.77	3182.9	4.57	8.20	3182.2	3.89	79.27	3135.0	7.22	13.30	3135.9	5.68	93.67	
3290.7	10.83	29.35	3297.9	12.35	21.59	3184.6	2.17	81.08	3188.7	5.15	7.41	3138.6	2.96	97.29	3147.2	7.04	11.93	
3312.4	2.33	56.23	3313.5	2.17	55.74	3211.6	0.00	54.00	3212.1	0.00	53.66	3158.5	0.17	62.29	3159.2	0.13	61.66	
3322.5	3.03	38.95	3323.6	2.89	39.78	3221.1	0.09	37.16	3221.9	0.06	37.96	3175.9	0.37	39.94	3176.9	0.31	41.04	
3437.1	16.72	37.43	3438.8	20.73	28.11	3305.1	15.82	43.21	3305.1	15.35	39.81	3281.7	16.82	44.32	3282.5	16.71	41.01	
3456.4	28.73	9.75	3439.2	16.81	35.61	3322.8	32.36	71.17	3312.6	39.79	21.70	3299.2	28.89	64.45	3288.6	32.52	24.93	
3460.5	0.54	107.78	3460.7	7.83	89.88	3331.2	16.26	72.84	3323.8	9.47	123.26	3306.7	12.65	74.12	3300.9	9.42	113.91	
scaling factor				0.914				0.995					0.992					

and 418.7 (1.21) cm^{-1} in the range 200–500 cm^{-1} . On the other hand, the planar EMI^+ gives four vibrations at 247.8 (0.67), 317.3 (0.08), 352.0 (0.47), and 443.6 (3.81) cm^{-1} . Note that the nonplanar EMI^+ is preferred to the planar EMI^+ . Comparison of the calculated vibrations and observed Raman bands is shown in Figure 4. It is supposed that the 230.1 (nonplanar) and 247.8 (planar) cm^{-1} vibrations may give the observed band at 241 cm^{-1} . Other bands observed at 297, 387, and 430 cm^{-1} are assigned mainly to vibrations at 291.6, 379.9, and 418.7 cm^{-1} , respectively, of the nonplanar conformer. Another observed band at 448 cm^{-1} may be assigned to the planar conformer, as the nonplanar conformer shows no vibration at that frequency; the plan

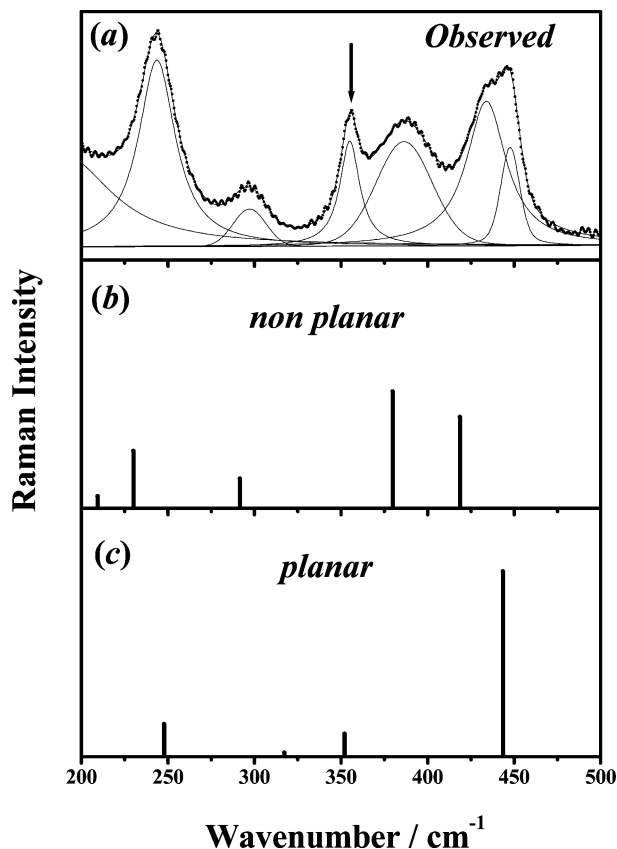


Figure 4. Raman spectra observed for $\text{EMI}^+\text{BF}_4^-$ over the frequency range 200–500 cm^{-1} (a) and theoretically predicted vibrations for the nonplanar (b) and planar (c) conformers of the EMI^+ ion. Theoretical Raman intensity is modified according to the population of nonplanar (0.61) and planar (0.39) conformers evaluated from MP2/aug-cc-pVDZ calculations. The arrow in a indicates a Raman band originating from BF_4^- .

(nonplanar) cm^{-1} bands are shown in Figure 5a, and those for the 448 (planar) and 430 (nonplanar) cm^{-1} bands are shown in Figure 5b. As seen, the $-R \ln(I_p/I_{np})$ values show no significant temperature dependence. The ΔH° values evaluated from the slope in Figure 5a are 2 and 2.1 kJ mol^{-1} in the $\text{EMI}^+\text{BF}_4^-$ and $\text{EMI}^+\text{CF}_3\text{SO}_3^-$ systems, respectively. The values 4 and 2.0 kJ mol^{-1} in the $\text{EMI}^+\text{BF}_4^-$ and $\text{EMI}^+\text{CF}_3\text{SO}_3^-$ systems, respectively, are also extracted from the slope in Figure 5b. If some uncertainties are taken into account, the ΔH° value is only slightly positive and is practically independent of the counter-anion. This means that the nonplanar conformer is slightly more stable than the planar one. It is plausible that the anionic environment hardly influences the conformational equilibrium, and geometry difference mainly determines relative stability of conformers in the liquid state. Indeed, the observed ΔH° values are in good agreement with the energy difference (corrected with zero-point energies) of the planar and nonplanar conformers, which lies in the range 1.9–3.6 kJ mol^{-1} depending on the level of theory employed.

Conclusion

The 1-ethyl-3-methylimidazolium (EMI^+) ion involves an ethyl group bound to the imidazolium N atom, and it was found that the ethyl group rotates along the C–N bond to yield conformers. The torsion energy potential surface for the rotation was theoretically evaluated. Two local minima with an energy difference of ca. 2 kJ mol^{-1} were found, suggesting that two conformers are present in equilibrium. Full geometry optimiza-

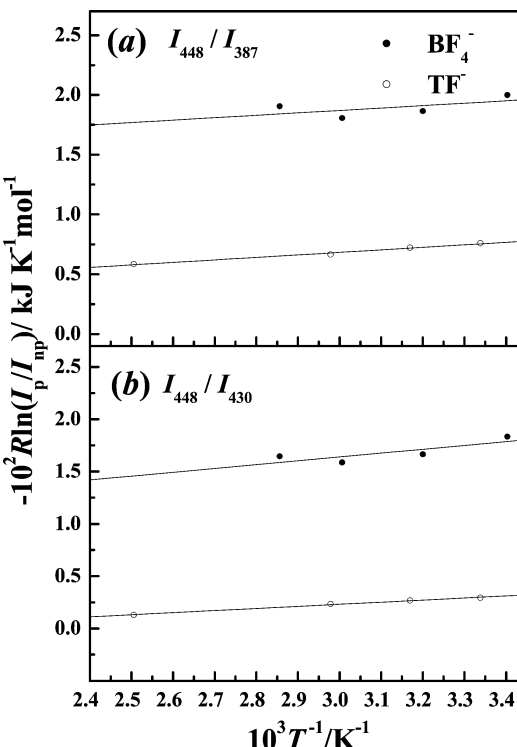


Figure 5. Plots of $-R \ln(I_p/I_{np}) / \text{kJ K}^{-1} \text{mol}^{-1}$ against $1/T$ for the planar (448 cm^{-1}) and nonplanar (387 cm^{-1}) bands (a) and for the planar (448 cm^{-1}) and nonplanar (430 cm^{-1}) bands (b). The slope gives the enthalpy for conformational change from nonplanar to planar.

tions followed by normal frequency analyses show that the two conformers are those with planar and nonplanar ethyl groups against the imidazolium ring plane, and the nonplanar conformer is slightly favored. The Raman spectrum of the EMI^+ in the range 200–500 cm^{-1} was investigated in detail. It is concluded that the EMI^+ shows five bands at 241, 297, 387, 430, and 448 cm^{-1} , the first four of which originate from the nonplanar conformer; the 448 cm^{-1} band originates from the planar conformer. The enthalpy for conformational change of the EMI^+ from nonplanar to planar was experimentally evaluated to be 2–4 kJ mol^{-1} , and the value is practically the same as that theoretically predicted. We thus conclude that the EMI^+ ion exists as either a nonplanar or planar conformer in the liquid EMI^+ salts and that the anionic environment hardly influences the equilibrium. The geometry difference between the conformers mainly determines their relative stabilities in the liquid state.

Acknowledgment. The authors wish to express their appreciation to the Nippon Synthetic Chemical Industry for providing special grade EMI salts. We also thank Prof. Y. Watanabe, Computing and Communications Center, Kyushu University, for his kind assistance with quantum chemical calculations. This work has been financially supported by Grant-in-Aids for Scientific Research 13440222 and 15750052 from the Ministry of Education, Culture, Sports, Science, and Technology of Japan, and also by a Grant for Basic Science Research Project from the Sumitomo Foundation.

Supporting Information Available: Partial atomic charges of nonplanar and planar EMI conformers at their optimized geometries, evaluated according to Mulliken, and atomic polar tensor and ChelpG methods based on MP2/aug-cc-pVDZ calculations are given in Table S1. Calculated band frequencies are plotted against observed ones over the range 200–1600 cm^{-1}

in Figure S1. The Cartesian coordinates for the optimized geometries will be given upon request. This material is available free of charge via the Internet at <http://pubs.acs.org>.

References and Notes

- (1) Rogers, R. D.; Seddon, K. R. *Ionic liquids as Green Solvents, Progress and Properties*; ACS Symposium Series 856; American Chemical Society: Washington, DC, 2003.
- (2) Adams, D. J.; Dyson, P. J.; Tavener, S. J. *Chemistry in Alternative reaction media*; John Wiley & Sons Ltd.: West Sussex, U.K., 2004.
- (3) (a) Hayashi, S.; Ozawa, R.; Hamaguchi, H. *Chem. Lett.* **2003**, *32*, 498–499. (b) Saha, S.; Hayashi, S.; Kobayashi, A.; Hamaguchi, H. *Chem. Lett.* **2003**, *32*, 740–741. (c) Ozawa, R.; Hayashi, S.; Saha, S.; Kobayashi, A.; Hamaguchi, H. *Chem. Lett.* **2003**, *32*, 948–949.
- (4) Holbrey, J. D.; Reichert, W. M.; Nieuwenhuyzen, M.; Johnston, S.; Seddon, K. R.; Rogers, R. D. *Chem. Commun.* **2003**, 1636–1637.
- (5) Wilkes, J. S.; Zaworotko, M. J. *J. Chem. Soc., Chem. Commun.* **1992**, 965–964.
- (6) Thirty-five crystal structures found in the CSD database are shown as their code in the CSD database as follows: BACQUS, BACRAZ, DIVGOE, DUVZAV, EGULOH, HAYBUE, HEDPUB, HERYOS, HER-YUY, HEZYOA, IBEDUO, IBEFAW, IBEFEA, IBEFIE, IBEFOK, KUCPED, KUCPIH, KUCPON, LIPFEV, LOBDEL, LOBDIP, LOBDOV, MIDHUC, PEVDEZ, PEVDID, PUHVET, QEKGUI, TETYUM, TEVFEF, TEVFII, UFAXAA, VEPFOL, XARROX, ZIBHUN, and ZIBJEZ.
- (7) Allen, F. H. *Acta Crystallogr.* **2002**, *B58*, 380–388.
- (8) Turner, E. A.; Pye, C. C.; Singer, R. D. *J. Phys. Chem. A* **2003**, *107*, 2277–2288.
- (9) Talaty, E. R.; Raja, S.; Storhaug, V. J.; Doille, A.; Carper, W. R. *J. Phys. Chem. B* **2004**, *108*, 13177–13184.
- (10) Lopes, J. N. C.; Deschamps, J.; Pádua, A. A. H. *J. Phys. Chem. B* **2004**, *108*, 2038–2047.
- (11) Liu, Z.; Huang, S.; Wang, W. *J. Phys. Chem. B* **2004**, *108*, 12978–12989.
- (12) (a) Hanke, C. G.; Price, S. L.; Lynden-Bell, R. M. *Mol. Phys.* **2001**, *99*, 801–809. (b) Shah, J. K.; Brennecke, J. F.; Maginn, E. J. *Green. Chem.* **2002**, *4*, 112–118. (c) De Andrade, J.; Boles, E. S.; Stassen, H. *J. Phys. Chem. B* **2002**, *106*, 3546–3548. (d) De Andrade, J.; Boles, E. S.; Stassen, H. *J. Phys. Chem. B* **2002**, *106*, 13344–13351. (e) Shim, Y.; Duan, J.; Choi, M. Y.; Kim, H. J. *J. Chem. Phys.* **2003**, *119*, 6411–6414. (f) Del Po'polo, M. G.; Voth, G. A. *J. Phys. Chem. B* **2004**, *108*, 1744–1752. (g) Urahata, S. M.; Ribeiro, M. C. C. *J. Chem. Phys.* **2004**, *120*, 1855–1863.
- (13) (a) Umebayashi, Y.; Matsumoto, K.; Mune, Y.; Zhang, Y.; Ishiguro, S. *Phys. Chem. Chem. Phys.* **2003**, *5*, 2552. (b) Ishiguro, S.; Umebayashi, Y.; Kanzaki, R. *Anal. Sci.* **2004**, *20*, 415–421. (c) Umebayashi, Y.; Mune, Y.; Tsukamoto, T.; Zhang, Y.; Ishiguro, S. *J. Mol. Liq.* **2005**, *118*, 45–49. (d) Umebayashi, Y.; Mroz, B.; Asada, M.; Fujii, K.; Matsumoto, K.; Mune, Y.; Probst, M.; Ishiguro, S. *J. Phys. Chem. A* **2005**, *109*, 4862–4868.
- (14) Marquardt, D. W. *J. Soc. Ind. Appl. Math.* **1963**, *11*, 431.
- (15) Press, W. H.; Flannery, B. P.; Teukolsky, S. A.; Vetterling, W. T. *Numerical Recipes*; Cambridge University Press: New York, 1989.
- (16) Frisch, M. J.; Trucks, G. W.; Schlegel, H. B.; Scuseria, G. E.; Robb, M. A.; Cheeseman, J. R.; Montgomery, J. A., Jr.; Vreven, T.; Kudin, K. N.; Burant, J. C.; Millam, J. M.; Iyengar, S. S.; Tomasi, J.; Barone, V.; Mennucci, B.; Cossi, M.; Scalmani, G.; Rega, N.; Petersson, G. A.; Nakatsuji, H.; Hada, M.; Ehara, M.; Toyota, K.; Fukuda, R.; Hasegawa, J.; Ishida, M.; Nakajima, T.; Honda, Y.; Kitao, O.; Nakai, H.; Klene, M.; Li, X.; Knox, J. E.; Hratchian, H. P.; Cross, J. B.; Adamo, C.; Jaramillo, J.; Gomperts, R.; Stratmann, R. E.; Yazyev, O.; Austin, A. J.; Cammi, R.; Pomelli, C.; Ochterski, J. W.; Ayala, P. Y.; Morokuma, K.; Voth, G. A.; Salvador, P.; Dannenberg, J. J.; Zakrzewski, V. G.; Dapprich, S.; Daniels, A. D.; Strain, M. C.; Farkas, O.; Malick, D. K.; Rabuck, A. D.; Raghavachari, K.; Foresman, J. B.; Ortiz, J. V.; Cui, Q.; Baboul, A. G.; Clifford, S.; Cioslowski, J.; Stefanov, B. B.; Liu, G.; Liashenko, A.; Piskorz, P.; Komaromi, I.; Martin, R. L.; Fox, D. J.; Keith, T.; Al-Laham, M. A.; Peng, C. Y.; Nanayakkara, A.; Challacombe, M.; Gill, P. M. W.; Johnson, B.; Chen, W.; Wong, M. W.; Gonzalez, C.; Pople, J. A., *Gaussian 03*, revision B.04; Gaussian, Inc.: Wallingford, CT, 2004.
- (17) Woon, D. E.; Dunning, T. H., Jr. *J. Chem. Phys.* **1993**, *98*, 1358–1371.
- (18) (a) Moller, C.; Plesset, M. S. *Phys. Rev.* **1934**, *46*, 618. (b) Head-Gordon, M.; Pople, J. A.; Frisch, M. J. *Chem. Phys. Lett.* **1988**, *153*, 503. (c) Frisch, M. J.; Head-Gordon, M.; Pople, J. A. *Chem. Phys. Lett.* **1990**, *166*, 275. (d) Frisch, M. J.; Head-Gordon, M.; Pople, J. A. *Chem. Phys. Lett.* **1990**, *166*, 281. (e) Head-Gordon, M.; Head-Gordon, T. *Chem. Phys. Lett.* **1994**, *220*, 122. (f) Saebo, S.; Almlof, J. *Chem. Phys. Lett.* **1989**, *154*, 83.
- (19) Becke, A. D. *J. Chem. Phys.* **1993**, *98*, 5648.
- (20) (a) Lee, C.; Yang, W.; Parr, R. G. *Phys. Rev. B* **1988**, *37*, 785. (b) Miehlich, B.; Savin, A.; Stoll, H.; Preuss, H. *Chem. Phys. Lett.* **1989**, *157*, 200.
- (21) (a) Mulliken, R. S. *J. Chem. Phys.* **1955**, *23*, 1833. (b) Mulliken, R. S. *J. Chem. Phys.* **1962**, *36*, 3428.
- (22) (a) Person, W. B.; Newton, J. H. *J. Chem. Phys.* **1974**, *61*, 1040. (b) Cioslowski, J. *J. Am. Chem. Soc.* **1989**, *111*, 8333.
- (23) Breneman, C. M.; Wiberg, K. B. *J. Comp. Chem.* **1990**, *11*, 361.